Conductive-tether design for de-orbiting from given altitude and inclination

Juan R. Sanmartin, Shaker B. Khan

Abstract— A bare tether with thin-tape cross section is both i) the most effective electrodinamic tether for given length and mass, and ii) capable of effective design for an arbitrary mission through its three disparate dimensions. It handily beats the fully insulated tether that exchanges current at both ends, a result resting in advantages of 2D current collection as against 3D collection; it has much greater perimeter than the round bare tether and much lower fatal debris-impact rate, leading to greatly faster de-orbiting and greatly higher probability of survival; and it only allows multi-line tethers reaching a few hundred lines to stand competitive. In selecting the disparate values of length *L*, width *w*, and thickness *h* for a de-orbit mission, performance involves three criteria: a) tether-to-spacecraft mass ratio must be small; b) probability of survival against the debris environment must be high; and c) de-orbiting must be fast to reduce manoeuvres for avoiding catastrophic collisions with big active/passive satellites around. Beyond determining tether mass through the product *Lwh*, main dimension parameters affecting performance are $L/h^{2/3}$ characterizing ohmic effects, and *w* determining electron collection. An algorithm for optimal selection of tape dimensions is elaborated.

Keywords— *Space debris, electrodynamic tethers, tether design*

I. INTRODUCTION

Future satellites should incorporate a de-orbit system to be used at end of mission to rein the risk in setting up the well-known Kessler cascade in space debris, as a constant menace to operative satellites in Low Earth Orbit (LEO) [1]. A de-orbiting technology, if repeatedly demonstrated, would facilitate international agreement on the more complex but required Active Debris Removal operation. Electrodynamic bare tethers, which are very light, propellantless, and passive systems, might effectively remove both future and current non-active satellites [2]-[6].

Several tether experiments have been flown in the past to analyze current collection, attitude control, and hollow-cathode operations. Failure due to a cut by space debris, however, is still an open issue because two past in-orbit experiments with round tethers, the SEDS-2 and TIPS missions, gave opposite results [7]. In addition, recent results showed that tape tethers have much greater survival probability than round tethers of equal length and mass, because they both de-orbit faster and have lower fatal-impact rate [8].

Juan R. Sanmartin and Shaker B. Khan are with E.T.S. Ingenieros Aernauticos, Universidad Politécnica de Madrid, 28040 Madrid, Spain. (e-mail: juanr.sanmartin@upm.es)

Tether geometry has thus a relevant impact on performance of the system, and tape tethers are quite advantageous in this respect; in particular, multi-line tethers would need have hundreds of lines to reach the current-capture perimeter of a tape of equal length and mass. Given a de-orbit mission, i e. initial orbital parameters and mass M_s of the satellite, one might choose tape length *L*, width *w*, and thickness *h* to optimize some figure of merit.

Opposite requirements of both a light tether and survivability against debris suggest a design scheme based on the dimensionless product Π of probability N_f of a cut and tether-to-satellite mass ratio m_t/M_s which should be kept to a minimum for an optimally designed tether. The present work explicitly shows Π as functional of tether geometry and orbital parameters, derived by combining a fatal-impact rate model introduced in [9] and a simple satellite dynamical equation that assumes a slow de-orbit evolution as sequence of near-circular orbits due to Lorentz drag on tether current induced by the geomagnetic field **B**. Since time is eliminated when combining both equations, Π is independent of tether de-orbit history and just depends on mission constraints (initial altitude and inclination) and tape dimensions *L, w,* and *h*.

Tether systems appear to dominate deorbiting technology for a broad range of parameters, including high-inclination orbits, an unfavorable condition, in principle, because the induced current might be too low. This issue is here illustrated by applying the design algorithm to a hypothetical mission for deorbiting a satellite at the orbit of Cryosat, an operative Earth-observing satellite following a non-synchronous orbit at 720 km altitude with inclination of 92 degrees, launched in April 2010 to measure artic sea-ice thickness.

In Secs. II and III the tether survival probability model obtained in [9] and the deorbiting dynamical equation are presented, respectively. These results are combined in Sec. IV to obtain the function Π. An application of the optimization algorithm is shown and conclusions are summarized in Sec. V.

II. SURVIVAL AGAINST DEBRIS

The long and thin geometry of tethers make them prone to fatal impacts by abundant small debris. As already mentioned, results found by Khan and Sanmartin show, however, that thin-tape tethers have much greater survival probability than round tethers of equal length and mass [8]. High survival probability over some de-orbit time Δt_d requires low fatal-impact count N_c in a Poisson probability distribution

$$P \approx \exp(-N_c) \approx 1 - N_c \qquad (1)$$

where N_c is simply related to a fatal count-rate, if at constant conditions, $N_c / L\Delta t_d$, a value $N_c = 0.05$, say, meaning that 5 among 100 tethers would be cut during deorbiting.

For the simplest case of a round tether of diameter D, a standard approximation for the fatal impact rate reads

$$\frac{dN_c}{dt} = -\int_{\delta_{m(D)}}^{\delta_\infty} \frac{dF}{d\delta} d\delta \times LD_{eff}(D, \delta), \qquad (2)$$

where $F(\delta, H, i)$ is the cumulative flux down to debris size δ, at given orbit altitude H and inclination i, by either ESA's MASTER or NASA's ORDEM flux models. In (2), δ_∞ is the largest relevant debris size, say 1 m, and $\delta_m(D)$ is the minimum size that may sever a tether. Energy considerations suggest $\delta_m \sim D/3$. The effective diameter, $D_{eff} = D + \delta - \delta_c$, with $\delta_c \sim \delta_m$, takes into account that debris have macroscopic size and that severing requires a minimum overlap of tether and debris volumes.

For tapes, the fatal impact rate involves an additional integral over impact angle between debris velocity and normal to the wide side of the tape. Using ESA's MASTER flux and a tape-tether, Khan and Sanmartin, making simple approximations, found an accurate analytical representation

$$\frac{dN_c}{dt} \equiv L\dot{n}_c \approx L \left[\frac{3n_0 + 2}{\pi(n_0 - 2)} \left(\frac{3\delta^*}{w}\right)^{n_0 - 1} \left(\sqrt{\frac{\pi w}{4h}}\right)^{n_0 - 2} - \frac{n_1 - n_0}{(n_1 - 1)(n_0 - 1)} \right] \delta^* F^* \qquad (3)$$

with n_0 and n_1 slopes in a log-log plot of F versus δ for power laws in two ranges $\delta < \delta^*$ and $\delta > \delta^*$, respectively [9]. The two straight lines in the log-log plot meet at the special point (δ^*, F^*).
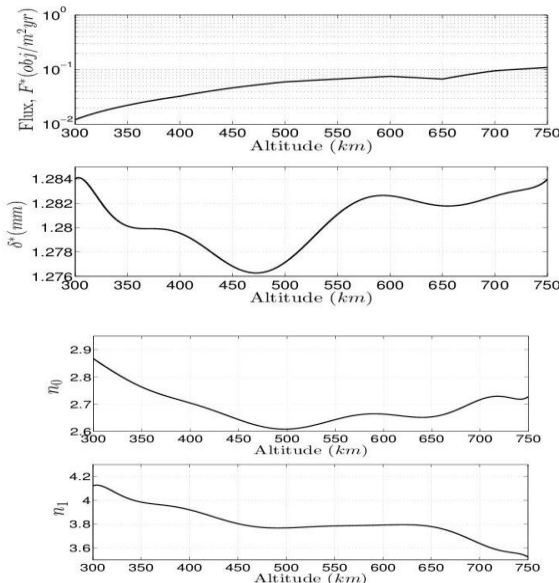

Fig. 1. Variations of MASTER model parameters n_0, n_1, δ^*, F^* are represented for a range of H values and given inclination of $92°$, appropriate for satellite Cryosat.

All four parameters in the model (n_0, n_1, δ^*, F^*) depend on orbit altitude and inclination. Fig. 1.shows an example of the dependence of these parameters on H at the inclination value $92°$. In all cases the particular debris diameter δ^* is close to 1 mm. For ORDEM, the debris flux rate would roughly be larger by one order of magnitude.

III. THE DE-ORBITING DYNAMICAL EQUATION

In the frame of an orbiting tether there is a motional electric field $\mathbf{E_m} = (\mathbf{v} - \mathbf{v_{pl}}) \times \mathbf{B}$ in the highly conductive ambient plasma around, with the near-corrotational $\mathbf{v_{pl}}$ plasma velocity negligible in LEO. This results in a not too wide bare tape collecting electrons over a segment coming out polarized positive, in the *orbital motion limited* regime [10]. Ion collection takes place over the complementary (cathodic) segment, at a comparatively low rate because of the high *ion-to-electron* mass ratio; the overall current balance thus requires a plasma contactor, typically a Hollow Cathode (HC), to eject electrons at the cathodic end.

Both tether bias and current I vary along the tether and are computed by solving a boundary value problem [11]. Current will be negligible if $\mathbf{E_m}$ points to the HC, where electrons must be emitted. For a prograde (retrograde) orbit and $\mathbf{u_t}$ the upwards vertical unit-vector the projection $E_m = \mathbf{u_t} \cdot \mathbf{E_m}$ is positive (negative) respectively. Assuming the tether aligned with the local vertical, the HC must be placed at the bottom (top) for prograde (retrograde) orbits. In the important case of high inclinations, say, from $80°$ to $100°$, the motional field E_m changes sign as the Earth rotates under the orbital plane; only for the daily fraction where it has the right direction there is sensible current. Most of the time E_m is positive (negative) for mostly prograde (retrograde) orbits; Fig. 2 shows a schematic of tether operation with the motional field reversing direction over a slightly retrograde (inclination $> 90°$) orbit.

Neglecting the HC potential drop and ion collection, the length-averaged current along the tether I_{av}, normalized by the short-circuit value, $I_{sc} = \sigma_c hwE_m$,

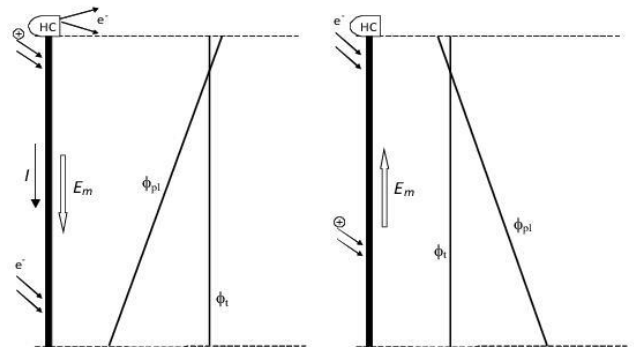$$I_{av} / I_{sc} \equiv i_{av}(\xi) \qquad (4)$$

Fig. 2 Schematic of tether operation with the motional field reversing direction during a near polar, mostly retrograde orbit, with the hollow-cathode correctly placed at the top. For simplicity in the figure, ohmic effects are assumed negligible, leading to a potential profile constant along the tether; ϕ_t and ϕ_{pl} are tether and faraway plasma potentials.

(Abstract No# (185)

is a definite function of a ratio involving tether and ambient parameters [11],

$$\xi \equiv \frac{L}{h^{2/3}l^{1/3}}, \quad l \equiv \frac{9\pi^2}{128}\frac{m_e\sigma_c^2 E_m}{e^3 n_e^2} \approx 2.38\cdot 10^{18}\times \frac{E_m/(150V/km)}{\left(n_e/10^5 cm^{-3}\right)^2}(m) \quad (5)$$

with σ_c tether conductivity and n_e ambient electron density. For $0 < \xi < 4$, $i_{av}(\xi)$ is exactly given by the implicit equation

$$i_{av} = 1 - \left[\int_0^1 \frac{d\varphi}{\sqrt{1+(1-i_{av})^{3/2}\,\xi^{3/2}\left(\varphi^{3/2}-1\right)}}\right]^{-1}, \quad (6)$$

which approaches $i_{av} = 0.3\xi^{3/2}$, for vanishing ξ, which is the no-ohmic effects limit, and keeps roughly accurate up to $\xi = 1$. For $2 < \xi < 4$ one may approximately write $i_{av} = 1 - 1/\xi$. This last expression is exact for $\xi > 4$.

For tape tether design analysis, we consider a mass point satellite with a rigid tether along the vertical, in a circular orbit weakly perturbed by the Lorentz drag $LI_{av}\ \mathbf{u}_t \wedge \mathbf{B}$. The equation of motion is

$$M_s\frac{d\mathbf{v}}{dt} + M_s\frac{\mu_E}{r^2}\frac{\mathbf{r}}{r} = LI_{av}\mathbf{u}_t \wedge \mathbf{B} \quad (7)$$

with μ_E the Earth's gravitational constant and $\mathbf{r}$ the position vector. The Lorentz drag makes the orbit slowly evolve through a long spiraling sequence of quasi-circular orbits. Carrying out the scalar product with $\mathbf{v} = d\mathbf{r}/dt$ in (7) we have

$$-M_s v\frac{dv}{dt} = -\sigma_c E_m^2 whLi_{av} \quad (8)$$

where we used $\mathbf{v}\cdot(\mathbf{u}_t\wedge \mathbf{B}) = -E_m$.

IV. CONDUCTIVE TETHER DESIGN FORMULA FOR A GENERIC MISSION

Equation (8) can be rewritten as an equation of evolution for the orbit-altitude H by using $v^2 \approx v_{orb}^2 = \mu_E/(R_E + H)$ with R_E the Earth radius, and introducing tether density, $\rho_t = m_t/Lwh$,

$$\frac{M_s}{m_t}\frac{dH}{dt} = -2(R_E + H)\frac{\sigma_c E_m^2}{\rho_t v^2}\times i_{av}(\xi), \quad (9)$$

which will hold over the fraction f_τ of orbital period having the motional field pointing away from the hollow cathode. We will take this into account by daily averaging (9) over the orbits and introducing a factor f_τ on the right hand side. Outside the inclination range $80°$-$100°$ one may set $f_\tau = 1$.

Combining the tether survival and deorbiting equation models we now derive a design formula for a generic mission. Introducing the length $s \equiv L^3/h^2 \equiv \xi^3 l$, and using (3) and (9) to divide dN_c/dt by dH/dt, there results an equation for the rate dN_c/dH,

$$\frac{m_t}{M_s}\frac{dN_c}{dH} \equiv \frac{L/2}{R_E+H}\frac{\rho_t v^2}{\sigma_c E_m^2}\frac{1}{f_\tau i_{av}}$$

$$\times \left[\frac{3n_0+2}{\pi(n_0-2)}\left(\frac{3\delta^*}{w}\right)^{n_0-1}\left(\sqrt{\frac{\pi w}{4h}}\right)^{n_0-2} - \frac{n_1-n_0}{(n_1-1)(n_0-1)}\right]\delta^* F^* \quad (10)$$

from the initial altitude H_0 to some final altitude H_f, there results an equation for the product of N_f (final value of N_c) and m_t/M_s, which we wish minimized,

$$\frac{m_t}{M_s}\times N_c = \Pi(w,h,L,H_0,i) \equiv \Pi(w,h,s,H_0,i) \quad (11)$$

$$\Pi \equiv \int_{H_f}^{H_0}\frac{dH(R_E+H_f)}{2f_\tau(R_E+H)^2}\frac{\rho_t v_f^2}{\sigma_c E_m^2}(y)\times \frac{\xi(s,H)}{i_{av}[\xi(s,H)]}\times l^{1/3}(H)h^{2/3}\times$$

$$\times \left[\frac{3n_0+2}{\pi(n_0-2)}\left(\frac{3\delta^*}{w}\right)^{n_0-1}\left(\sqrt{\frac{\pi w}{4h}}\right)^{n_0-2} - \frac{n_1-n_0}{(n_1-1)(n_0-1)}\right]\delta^* F^* (m^{-2}y^{-1}) \quad (12)$$

where $v_f = \sqrt{\mu_E/a_f}$ is the final velocity of the satellite, the ratio $\rho_t v_f^2/\sigma_c E_m^2$ is a characteristic time, and parameters F^*, δ^*, n_0 and n_1 are functions of orbital altitude and inclination, as given in Fig. 1 for the Cryosat inclination.

We remark that Π is time-independent and just involves tether geometry and orbit parameters. We consider de-orbiting down to $H_f = 300$ km, where air-drag on the reasonably large tether surface area $\sim Lw$, typically results in rapid reentry, while plasma density decreases below the ionospheric F layers. An important feature of the design formula (12) is the ratio ξ/i_{av}, which is just a function of the dimensionless variable ξ. Fig. 3 shows curves of ξ, i_{av} and ξ/i_{av} for a range of ξ values. The indefinite increase of the ratio ξ/i_{av} inside the integral for small and large ξ will lead to some minimum of Π.
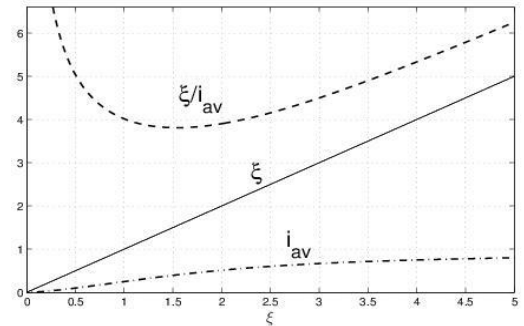

Fig. 3 Curves of ξ, i_{av} and ξ/i_{av} are represented for a range of ξ values.

(Abstract No# (185)

V.   DISCUSSION OF RESULTS

Carrying out the integral defining Π in (12) requires setting the initial altitude H_0 and inclination i, 720 km and 92° for the Cryosat case. It next involves 7 daily-averaged profiles in altitude H, the parameters given in Fig. 1 and two ambient plasma profiles E_m and l (dependent on both E_m and n_e) from the international IGRF and IRI models for **B** and n_e. They are given in Fig. 4, also showing the orbit factor f_τ.

An averaged solar flux of several 11-years cycles is considered for the ambient models. Notice that higher (lower) solar flux would make the electron density increase (decrease). The average current I_{av}, increasing with n_e, would then increase and decrease for high and low solar flux, respectively. For the retrograde Cryosat-like orbit here studied the daily-averaged field E_m is negative about 53-54 %   (f_τ = 0.53-0.54). Numerical results for Π are shown in Fig. 5 for a range of w and $s(L, h)$ values.

Note that with the second term in the square bracket in (12) comparatively small, and n_0 presenting a nearly constant value in Fig. 1, Π follows approximate power law in both w and h, showing very little dependence on h. As regards the length $s = L^3 / h^2$, Π increases very fast with decreasing $s^{1/3}$ to the left of, say, 0.5, and varies very little to its right. Also, splitting Π into its factors N_f and m_t / M_s might depend on the type of mission. Finally, recalling that the ORDEM model would yield rates dN_c / dt one order of magnitude larger, and setting N_f = m_t / M_s, ORDEM would yield a mass fraction about 3 times larger.
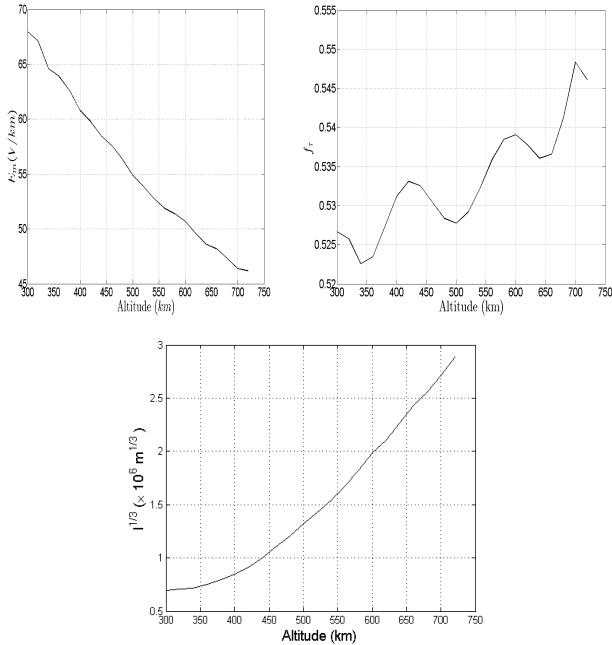

Fig. 4 Profiles of E_m, $l^{1/3}$ and f_τ for Cryosat (H_0 = 720 km, i = 92 deg). The daily-averaged field E_m is negative about 53 %.
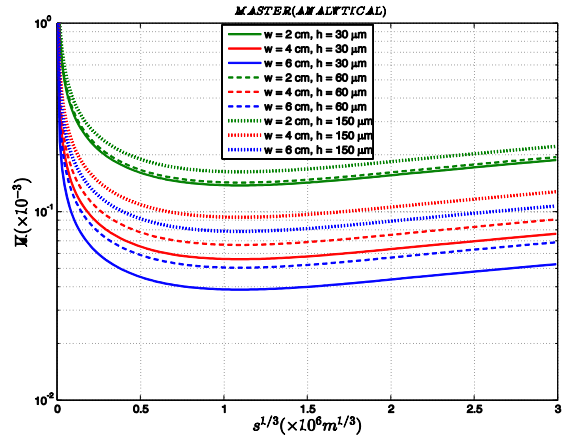

Fig. 5 Numerical results for Cryosat, Π given for a range of w and $s \equiv L^3 / h^2$ values.

ACKNOWLEDGMENT

REFERENCES

[1]   D.J. Kessler and B.G. Cour-Palais, "Collision frequency of artificial satellites: The creation of a debris belt", Journal of Geophysical Research, vol.83, pp. 2637-2646, 1978.

[2]   R. L. Forward, R. P. Hoyt, and Uphoff C., "The Terminator tether: A near-term commercial application of the NASA/MSFC ProSEDS experiment", *Proceedings of the Tether Technology Interchange Meeting*, NASA CP-1998-206900, 1998, p. 109.

[3]   E.J. Van der Heide and M. Kruijff, "Tethers and debris mitigation", Acta Astronautica, vol. 48, pp. 503-516, 2001.

[4]   E.Ahedo and J.R.Sanmartin,"Analysis of bare-tether systems for deorbiting LEO satellites", Journal of Spacecraft and Rockets, vol. 39, pp. 198-205, 2002.

[5]   B. Gilchrist, B. Lim, N. Meckol, R. Masse, and S. Williams, "The use of electrodynamic tethers for orbit maintenance and deorbit of large spacecraft: A trade study of the NASA GLAST mission", 38th AIAA/ASMESAE/SEE *Joint Propulsion Conference Meeting and Exhibit*, AIAA Paper 2002-4044, July 2002.

[6]   C. Pardini, T. Hanada, and P.H. Krisko, "Benefts and risks of using electro-dynamic tethers to de-orbit spacecraft", Acta Astronautica, vol. 64, pp. 571-588, 2009.

[7]   J. A. Carroll and J.C. Oldson, "Tethers for small satellite applications", *AIAA/USU Small Satellite Conference*, Logan, Utah, 1995.

[8]   S.B. Khan and J.R. Sanmartin, "Survival probability of round and tape tethers against debris impact", Journal of Spacecraft and Rockets, vol. 50, pp. 603-608, 2013.

[9]   S. B. Khan, and J.R. Sanmartin, "Analysis of tape tether survival in LEO against orbital debris, Advances in Space Research, vol. 53, pp 1370–1376, 2014.

[10]   J.R. Sanmartin, and R.D. Estes, "The orbital-motion-limited regime of cylindrical Langmuir probes", Phys. Plasmas, vol. 6, pp. 395-405, 1999.

[11] J.R. Sanmartin, M. Martinez-Sanchez, and E. Ahedo, "Bare wire anodes for electrodynamic tethers", Journal of Propulsion and Power, vol. 9, pp. 353-360, 1993.

[12] J.R.   Sanmartin,   E.   Lorenzini,   and   M.   Martinez-Sanchez, "Electrodynamic tether applications and constraints", Journal of Spacecraft and Rockets, vol. 9, pp. 442-456, 2010.